

Effect of thermal treatment on the structure and texture of titania

S. A. SELIM*, CH. A. PHILIP, S. HANAFI
Faculty of Science, Ain Shams University, Cairo, Egypt

H. P. BOEHM
*Institute of Inorganic Chemistry, Technische Universität München, 8000 Munich 2,
Arcisstrasse 21, FRG*

Anatase and rutile pigments, from two sources (B and T) were thoroughly purified from sulphate and chloride contaminants, thermally treated in the temperature range 150 to 550°C, and investigated using thermogravimetric (TG), differential thermal analysis (DTA), X-ray diffraction (XRD), nitrogen and organic vapour adsorption techniques. TG analysis reveals two main dehydration steps, the first results from physically adsorbed water and the second from structural and ligand water. The number of ligand water molecules released through a unit surface area (nm²) is in the range 4.50 to 5.15, being evolved in the temperature range 250 to 300°C. Two dehydroxylation endotherms appear for the anatase samples in the temperature range 350 to 420°C which seem to arise from the presence of two types of hydroxyls. No transformation from the anatase to rutile structure occurred in the temperature range investigated. Estimation of crystallite sizes showed a marked increase at temperatures >250°C for anatase (B), being greatest for the (1 0 1) plane, and >400°C for rutile (B), where the three planes (1 0 1), (1 1 0) and (1 1 1) increased distinctly. Maximum anisotropy was observed for the anatase heated at 550°C. Nitrogen adsorption data revealed a marked decrease in the specific area and total pore volume by thermal treatment ≥400°C for anatase and ≥250°C for rutile whereby it retains a nearly stable \bar{r}_H value with an average range of 2.62 nm. The anatase (B) samples are composed of a mixture of both meso- and micropores whereas for rutile (B) microporosity appeared only for the sample heated at 150°C, becoming predominantly mesoporous at higher temperatures. Most heated samples exhibited two group sizes in the mesopore range resulting from their existence in the form of particles constituted from a collection of small particulates. The rutile (B) products are generally characterized by possessing a wider pore system than those from anatase. The anatase (T) samples are predominantly microporous at 150°C and become mesoporous at 550°C – the reverse is true for rutile (T). Cyclohexane and benzene adsorption measure only a fraction of the nitrogen area. Specific interaction (H-bonding) is believed to exist in some cases between the cyclohexane molecules and titania surface hydroxyls, as well as some enhanced adsorption which is believed to occur with benzene adsorbate.

1. Introduction

The wide industrial use of titania is fast increasing. Its use as a catalyst [1, 2] is advancing especially as a photo catalyst in oxidation processes [3, 4]. The activity of a catalyst is, in general, highly controlled by its preparation conditions that result in a product of suitable textural properties and high surface activity so as to enhance both the diffusion and catalytic processes of concern. However, hydroxylation of the oxide appears to have an important role in the photo-activity [5]. Several methods have been adopted for the preparation of pure titania gels of high surface area [6–10] but most industrial products are highly contaminated with sulphate or chloride anions that greatly interfere with the hydration of these gels. Although traces of these anions may participate in [11, 12] or

enhance [13, 14] some specific catalytic processes, they must still be incorporated under controlled experimental conditions.

To what extent these contaminants would impose an effect, whether directly or indirectly, on the texture and structure of TiO₂ has not yet been revealed. However, these properties are largely controlled by the nature of the water surrounding the titanium ions, that may be affected by the anions present which, upon its evolution, would give rise to a gel of modified surface and textural properties. This was the aim of the present investigation, where two titania modifications, anatase and rutile, were supplied by Bayer (West Germany) and Tioxide (UK) companies. These were highly purified from contaminants and the resulting titania gels are investigated using thermal

* Author to whom all correspondence should be addressed.

(thermogravimetry, differential thermal analysis), structural (X-ray) and textural (nitrogen and organic vapour adsorption) techniques.

2. Experimental procedure

Four titania samples were used in this investigation supplied by BTP Tioxide (T) International Ltd (UK) and Bayer (B) AG (West Germany). From the former, two titania pastes were used, quoted as 1136/1 (anatase) and 1136/3 (rutile) prepared from sulphuric and hydrochloric acid solutions, respectively. These pastes when supplied had a solid content of about 45% TiO_2 and their chemical analysis, given by Tioxide Ltd, showed a high SO_4^{2-} contamination of sample 1136/1 reaching $\sim 2.38\%$ (SO_3) and therefore needed purification.

Two samples were also supplied by Bayer, one was an anatase obtained from hydrolysed TiO_2 (Ta) and the other a rutile obtained from hydrolysed TiCl_4 (Tr).

All four samples were thoroughly cleaned to unify treatment conditions. The cleaning procedure was achieved by washing the solids with concentrated NaOH solution several times, followed by concentrated HCl solution until free from any sodium ions, and finally with distilled water until the concentration of Cl^- was $< 50 \mu\text{mol g}^{-1}$. The purified solid materials were then dried at room temperature and dehydration products were obtained by heating portions in the presence of air for 3 h at 150, 250, 400 and 550°C. The treatment temperature will always follow the sample symbol and the origin symbol, (B) or (T), will be used when necessary.

Thermogravimetric analysis (TGA) was carried out in the presence of static air using a Stanton Redcroft Thermobalance type 750/770 connected to a BD9 two-channel automatic recorder (Kipp and Zonnen) at a heating rate of $10^\circ\text{C min}^{-1}$.

The differential thermal analysis (DTA) was carried out using an apparatus from Netzsch Gerätebau GmbH Selb (Bavaria) no. 348 472C, using α -alumina as reference material. The heating rate was also $10^\circ\text{C min}^{-1}$.

The XRD patterns were obtained using a Philips X-ray diffractometer unit model PM 9920/05 using nickel-filtered $\text{CuK}\alpha$ radiation. The d distances were calculated and, with their relative intensities, were compared with data in the ASTM cards [15, 16].

The adsorption-desorption isotherms of nitrogen at -195°C and of cyclohexane and benzene at 35°C were determined by conventional volumetric gas adsorption apparatus, adopting the appropriate cross-sectional area, A_m .

3. Results and discussion

3.1. Structural characteristics

3.1.1. Thermal analysis

TGA showed that the dehydration of both titania modifications takes place in two main steps (Fig. 1). The first step results mainly from physically adsorbed water and terminates in the temperature range 180 to 290°C depending on the type, origin and porosity of the TiO_2 . From the magnitude of the percentage loss of the first step, the anatase samples Ta and 1136/1 are

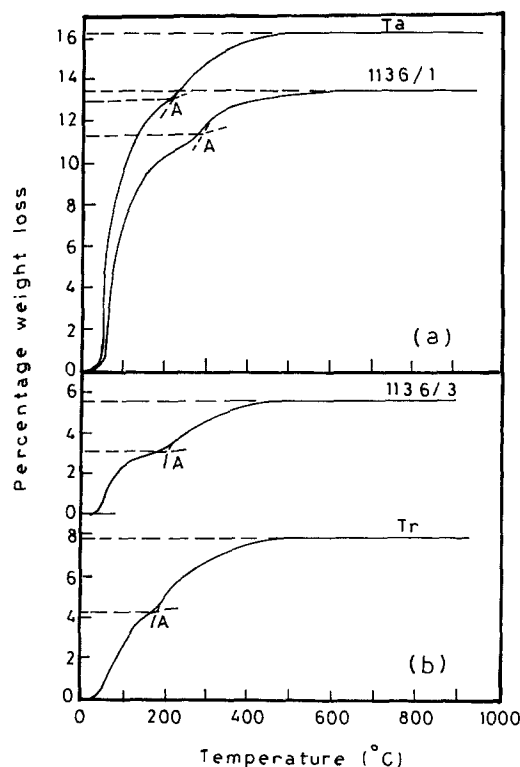


Figure 1 Thermogravimetric curves for the (a) anatase and (b) rutile samples.

found to possess in excess of three times more physically adsorbed water than the corresponding rutile samples Tr and 1136/3. This increased amount of physically adsorbed water may arise from (i) an increase in the net surface charges arising from an increase in the polarity of the surface ions, (ii) the uptake of water as ligand water to complete the coordination of the titanium ion in the oxide which may differ in the anatase samples from the rutile samples, in which case it may either be evolved at low or high temperatures depending on its stability, and (iii) large surface area probably resulting from the presence of micropores. We are inclined to believe that the last factor, the high specific area, is the major contributing factor to this increased physisorbed water. This can be tested roughly by comparing the values obtained for (i) the ratio between the percentage losses and (ii) that of their corresponding areas obtained for samples heated at the termination of this step – nearly identical results are expected to result if the specific area is the main contributing factor. The specific areas arbitrarily employed here are those obtained at 150°C assuming that treatment for 3 h at this temperature produces a comparable dehydration effect to that at a slightly higher temperature. Samples heated at 250°C showed very low surface areas where low-temperature sintering may have taken place and therefore could not be employed here, as completely erroneous results would be obtained. Accordingly, the ratio for the first TG step is 0.33 compared to a value of 0.43 for Tr and Ta, and for samples 1136/3 and 1136/1 values of 0.28 and 0.36 are obtained. The small discrepancy observed in the values of the area ratios is expected, because they are taken arbitrarily for the samples heated at 150°C and the termination of the first TG step of the anatase samples is located at a higher

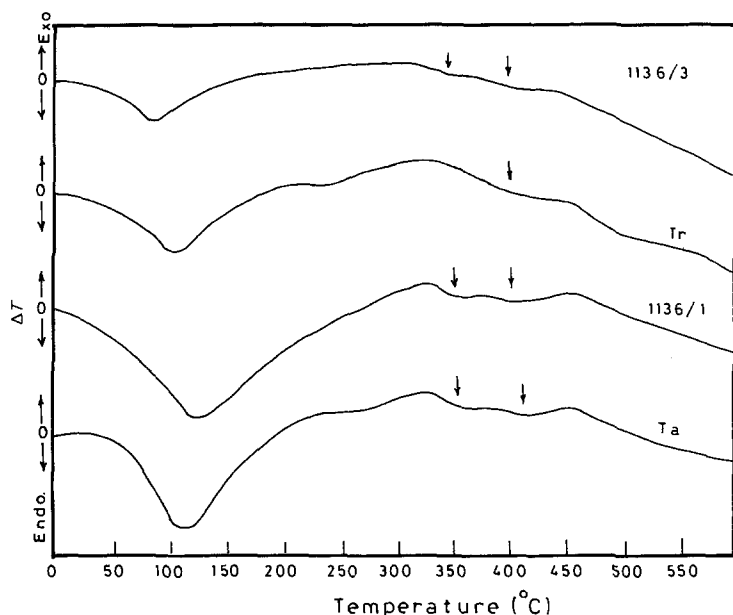


Figure 2 Differential thermal analysis curves of the anatase (Ta, 1136/1) and rutile (Tr, 1136/3) samples.

temperature than that for the rutile samples, so that slightly higher area values would be expected for these anatase samples.

Therefore, the increased adsorption of water in the first step of the anatase samples results from its possession of high specific surface area; actually these samples contain micropores (revealed later).

The second dehydration step mainly arises from the dehydroxylation of titania together with some strongly bound water. Comparable loss values are observed for both modifications with those from (B) slightly in excess (Table I, column 4).

To identify the nature of the evolved water from this step, the number of OH groups/nm² is calculated according to the method given by Vleeskens [17] and compared with that evaluated by H-D exchange carried on the same samples [18] and which is believed to give the total surface OH groups.

Because the first step is mainly concerned with physically adsorbed water, the drying temperature of our samples should be taken as that at the termination of the first step. Also the ignition temperature is taken at 800°C which is far above the evolution of the last traces of water. The surface area value, S^{N_2} substituted in Vleeskens' equation is that obtained for the sample heated at 150°C. The number of OH groups so calculated for samples Tr and 1136/3, give values of 21.6 OH/nm² and 22.6 OH/nm², respectively (Table I, column 6). These values are, in fact, much higher than those obtained by H-D exchange being 12.6 and 12.3 OH/nm², respectively. A fully hydroxylated TiO₂

surface is believed to have 12 to 14 OH/nm² [19, 20] which indicates the presence of some other type of strongly bound water which is only evolved at a temperature range located within that of the second step. If the number of OH groups evaluated by H-D exchange is subtracted from the corresponding values obtained by TGA, we obtain the number of OH groups arising from the bulk or from this differently bound water, and evolved through a surface of 1 nm², being 9.0 and 10.3 for samples Tr and 1136/3, respectively, and corresponding to 4.50 and 5.15 water molecules (columns 7 and 8).

As titanium in the titanium oxide lattice can accommodate ligand water to complete its coordination shell, it is plausible to believe that this excess number of OH groups (or water molecules) actually arises from the evolution of this ligand water whose presence was also noticed by others [10, 19]. Thus the second step in the TG curves results from the presence of molecular water present as ligand water and the hydroxyl groups, whatever their nature. However, one should not neglect the possibility that the water adsorbed by two hydrogen bonds (physically adsorbed) could be evolved at slightly higher temperatures, nevertheless, one would not expect it to take place at temperatures above 150°C in analogy to what was observed with silica gel [21].

The results for the anatase samples should be taken with reservation as the termination of the first step is above 200°C for both samples (Fig. 1). S^{N_2} employed for sample Ta (158.1 m²g⁻¹) is that obtained at 250°C

TABLE I Percentage losses as evaluated from TG curves for the different steps together with the number of OH groups evaluated according to Vleeskens' method

Sample	$S_{BEI}^{N_2}$ -150 (m ² g ⁻¹)	% loss of first step	% loss of second step	% loss of second step referred to dry matter	Total OH/nm ² Vleeskens' method	Excess evolved OH/nm ²	Number of water molecules evolved in excess to the surface OH
Ta	254.6	13.00	3.24	3.87	17.9	17.9 - (8.8)* = 9.1	4.55
1136/1	212.6	11.30	2.10	2.42	-	-	-
Tr	109.5	4.30	3.60	3.91	21.6	21.6 - (12.6)* = 9.0	4.50
1136/3	76.7	3.15	2.45	2.59	22.6	22.6 - (12.3)* = 10.3	5.15

*Values taken from H/D exchange.

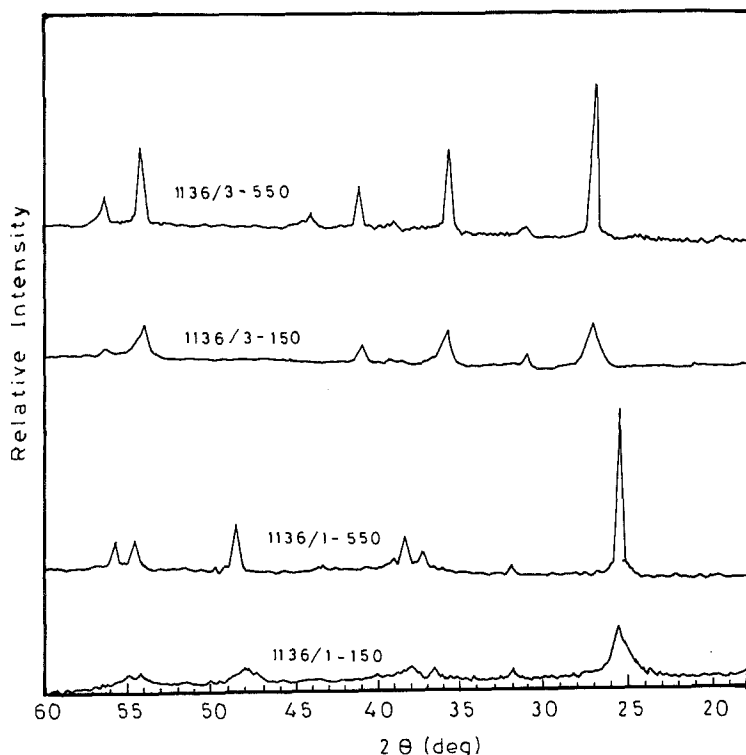


Figure 3 X-ray diffraction patterns for the thermal products of the two titania modifications from Ti oxide.

which is slightly above the termination of the first step, whereas no area measurements were evaluated at this temperature for sample 1136/1.

Thus for sample Ta the total number of OH/nm² according to Vleeskens' method is 17.9 and as the results from H-D exchange give 8.8 OH/nm², then 9.1 OH groups/nm² arise from the ligand water giving 4.55 water molecules. This value is comparable with that obtained for sample Tr (Table I, column 8).

The DTA curves obtained for the titania samples show much similarity between those of anatase and rutile, differing only in the intensity and location of the observed peaks (Fig. 2). The first step in the TGA curves characterizing physically adsorbed water is reproduced in the corresponding DTA curves as a large endotherm in the temperature range 95 to 127°C, being larger for the anatase samples. In the case of the Bayer samples, and irrespective of modification, a small and very broad endotherm is noticed in the temperature range 250 to 300°C that seems to result from the evolution of ligand water, being evolved prior to the dehydroxylation of the surface.

For the Ti oxide samples, this endotherm is not distinct due to its overlap with the preceding large endotherm resulting from the physisorbed water. Two other small endotherms clearly appear for the anatase samples, being centred in the temperature range 350 to 420°C, that are less pronounced for the rutile modification. They are believed to be responsible for the dehydroxylation of the titania surface and may possibly be considered to indicate the presence of two types of hydroxyls usually present in the titania surface [22, 23].

At about 455°C, a small broad exothermic peak is observed which results from a sintering or agglomeration process and is commonly noticed with oxide systems [21, 24].

3.1.2. X-ray analysis

The X-ray diffraction patterns of the heated products at temperatures up to 550°C of samples Ta and Tr show that they acquire their usual crystalline pattern [15, 16] — thermal treatment increases their crystallinity, where the peaks become sharper. The X-ray patterns obtained for samples 1136/1 and 1136/3 point to a crystallinity lower than those of Ta and Tr, but it is greatly improved upon heating to 550°C. Samples thermally treated at > 400°C exhibit a small peak at a distance 0.2338 nm (1 1 2 plane) and 0.2291 nm (2 0 0 plane) for the anatase and rutile samples, respectively. Fig. 3 shows the X-ray patterns obtained for the Ti oxide samples heated at 150 and 550°C for both modifications.

Of special interest is the variation of crystallite size with treatment temperature of samples Ta and Tr, calculated from the X-ray broadening of the peaks by applying the formula [25] for line broadening by crystals of size L , given as $L = K\lambda/\beta \cos \theta$, where λ is the wavelength of X-ray radiation, K is usually taken as 0.94 and approximated to 1, β is the line width at half maximum height. The line width, β , is corrected for instrumental broadening by employing the patterns obtained for large-sized TiO₂ pigments under the same experimental conditions. The variation of the crystallite sizes for each plane with treatment temperature for both modifications is represented in Fig. 4. Upon heating the anatase sample Ta to 250°C, a small increase in the crystallite size is observed for the (1 0 1), (2 0 0), (2 1 1), and (0 0 4) planes that increases markedly for the (1 0 1) and (2 0 0) planes upon further heating to 400°C.

A further increase in the crystallite size is observed above 400°C which is quite distinct for the (2 0 0) and (2 1 1) planes. It appears that in the anatase modification the small increase in crystallite size observed

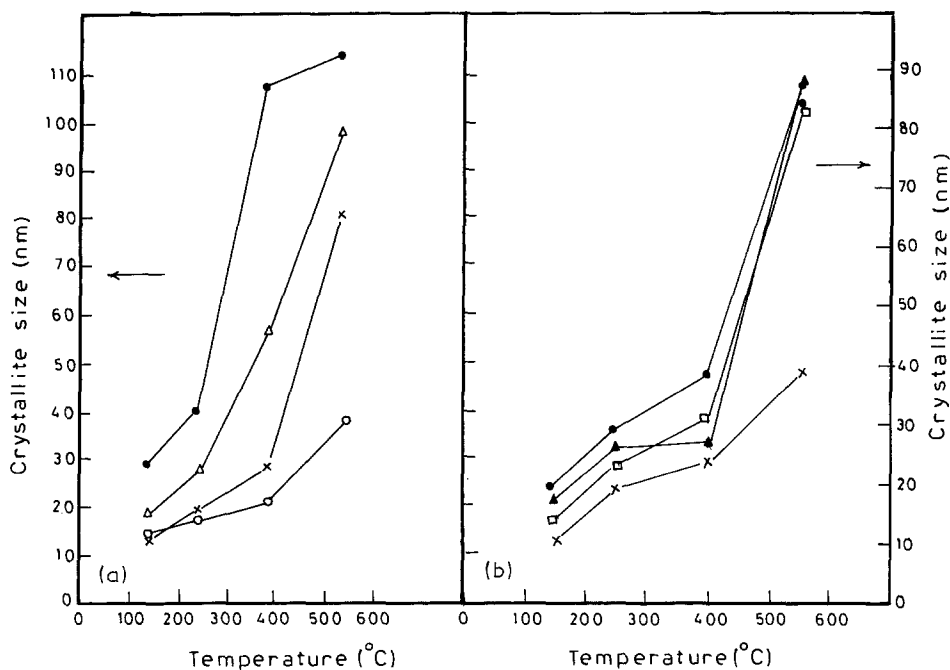


Figure 4 Variation of the crystallite sizes of the various planes with treatment temperature for samples (a) Ta and (b) Tr. (a) (●) 101, (Δ) 200, (x) 211, (○) 004. (b) (□) 110, (●) 101, (▲) 111, (x) 211.

below 250°C is a consequence of the release of the physically adsorbed water where the hydrogen bonding between them and the surface hydroxyls seems to have put the crystal planes under mild strain. As physically adsorbed water has no preference of one plane over the other, the increase in crystallite size is comparable for the various crystal planes taking into account the probability of one plane being preferentially exposed. Above 250°C, the increase in L becomes significant and results from the loss of ligand water and dehydroxylation. This large increase in L of the different planes in the temperature range 250 to 400°C may point to the preferred attachment of the OH groups to these planes and, therefore, to the probability of its exposure at the surface.

The normal process of expansion of the unit cell prior to the transformation to the rutile structure usually occurring above 600°C [26] should not be ignored.

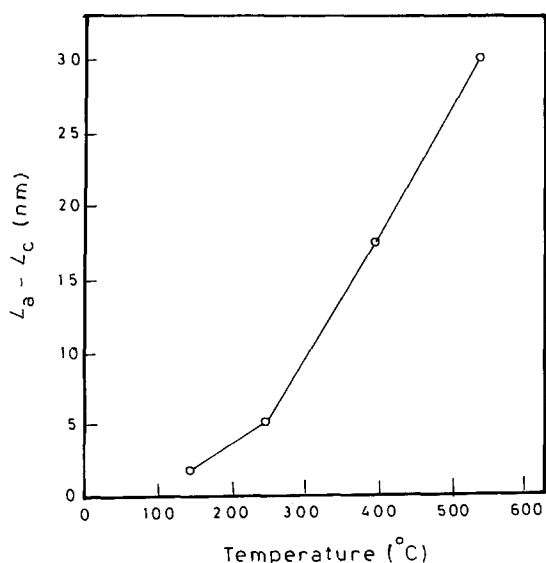


Figure 5 Variation of the differences in the crystal planes between the a and c directions with treatment temperature for sample Ta.

For rutile a gradual increase is observed in the crystallite size of the various planes with treatment temperature up to 400°C above which a marked increase results especially for the (101), (110) and (111) planes (Fig. 4).

Comparing L_a and L_c values from $(hk0)$ and $(00l)$ reflections actually corresponds to comparing the crystallite dimension in the a and c directions, respectively. For the anatase sample, Ta, comparison of the crystal planes (200) and (004) for the heated product obtained at 150°C gives values of 8.79 and 6.93 for L_a and L_c showing the solid to be nearly isotropic. If the difference between both L dimensions ($L_a - L_c$) is drawn against temperature, the tendency towards anisotropy can be visualized and it can be seen that maximum anisotropy is observed for the sample treated at 550°C (Fig. 5). For the rutile samples the difference between L_a and L_c is quite small, which may result in misleading speculations.

3.2. Surface texture

3.2.1. Nitrogen adsorption

The adsorption isotherms of nitrogen obtained for all the heated products of both modifications are type II. The adsorption-desorption isotherms are all completely reversible except samples Ta-150, Tr-250 and Tr-400, which form closed hysteresis loops that close at relative pressures above 0.8 for sample Ta-150 and at intermediate values for the rutile samples.

The specific surface areas are estimated by the application of the BET equation over its normal range of applicability and by adopting a value of 1.62 nm as the molecular area of adsorbed nitrogen.

The surface area, $S_{\text{BET}}^{\text{N}_2}$, so obtained and the total pore volume, $V_{p,0.95}$ (evaluated as liquid adsorbate at a relative pressure of 0.95) of the anatase sample Ta decreases markedly on heating to 400°C as a result of dehydration and dehydroxylation processes (Table II, columns 3 and 5, respectively).

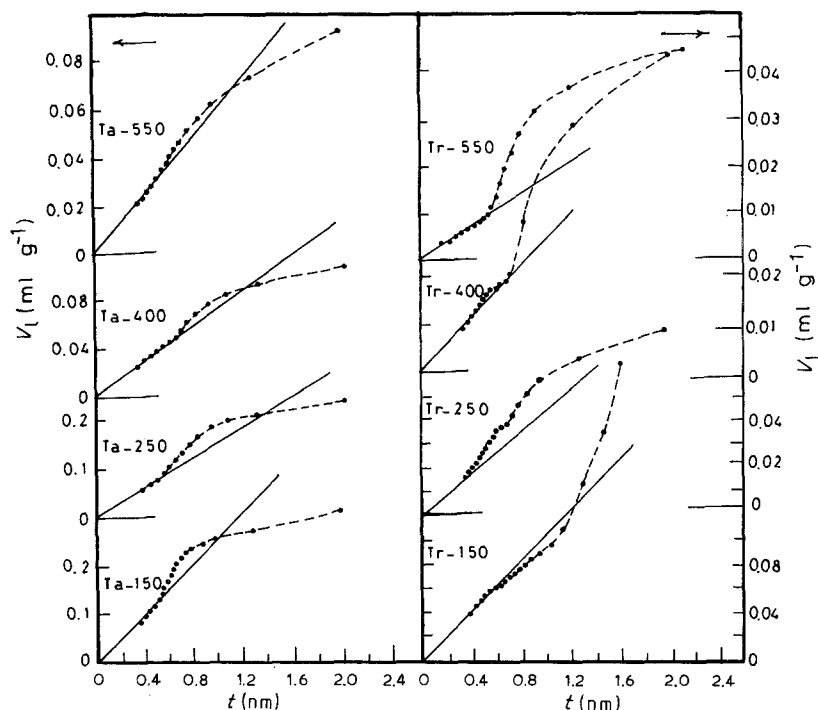


Figure 6 V_1-t plots obtained from nitrogen adsorption data on the heated products of sample Ta and Tr.

Above 400°C, a further and relatively smaller decrease takes place as a result of sintering. The average pore radius is only slightly affected above 150°C, possessing an average value of 1.48 nm (column 6). The products of the rutile sample Tr are mostly affected by heating to 250°C, where the specific surface area and total pore volume decrease and the average pore radius increases as a result of low-temperature sintering which follows the dehydration-dehydroxylation process (Table II). The average pore radius remains almost unchanged for products heated to $\geq 250^\circ\text{C}$, with an average value of 2.62 nm — shrinkage is believed to accompany the sintering process.

Both modifications of Ti oxide samples possess lower areas than the corresponding Bayer samples at 150°C only. At 550°C, the anatase modification, 1136/1, possesses a lower area and wider average pore radius than the corresponding Bayer sample, Ta-550. The reverse is true for the rutile modification 1136/3 that is found to possess a large specific area and a much smaller average pore radius relative to the corresponding sample from Bayer.

The pore system is identified by using the t -method of De Boer and co-workers [27, 28]. The $S_t^{\text{N}_2}$ values so obtained show good agreement with the correspond-

ing $S_{\text{BET}}^{\text{N}_2}$ values thereby indicating the suitable choice of t -curves [29–31] on the basis of the BET-C constant (Table II, columns 4 and 3, respectively).

From the V_1-t plots obtained, sample Ta-150 shows two regions of upward deviation at t -values of ~ 0.50 and ~ 0.60 nm that revert back at a t -value of ~ 1.0 nm showing the sample not only to be composed of a mixture of both meso and micropores, but also signifies the existence of two groups of pore sizes in the mesopore range (Fig. 6). At 250°C widening of the pore system takes place masking the presence of the two groups of mesopores and the plot reverts back at a t -value of ~ 1.36 nm. Some of the narrower pores seem to collapse upon evolution of water from them, leaving the system with wider pores as also reflected by the \bar{r}_H values (Table II, column 6). Heating to 400°C appears to bring about a process of pore narrowing, being reflected in the decrease observed in \bar{r}_H . This pore narrowing is a natural sequence of the marked increase observed in the crystallite size (Fig. 4). In this shrinkage of the pore system some of the narrower pores become inaccessible to the nitrogen molecules resulting in a marked decrease in both $S_{\text{BET}}^{\text{N}_2}$ and $V_{p0.95}$. Heating at 550°C causes widening of the pore system as a result of a further increase in crystallite size that

TABLE II Some surface characteristics of the heated products of Ta, Tr, 1136/1 and 1136/3 as obtained from nitrogen adsorption

Sample	BET C-constant	$S_{\text{BET}}^{\text{N}_2}$ ($\text{m}^2 \text{g}^{-1}$)	$S_t^{\text{N}_2}$ ($\text{m}^2 \text{g}^{-1}$)	$V_{p0.95}$ (ml g^{-1})	\bar{r}_H (nm)
Ta-150	86	254.6	258.0	0.3140	1.24
Ta-250	139	158.1	159.0	0.2363	1.49
Ta-400	295	74.3	75.0	0.1060	1.42
Ta-550	195	56.8	58.5	0.0863	1.54
Tr-150	201	109.5	108.0	0.1881	1.72
Tr-250	196	44.6	44.0	0.1166	2.61
Tr-400	92	27.6	26.0	0.0720	2.61
Tr-550	22	16.4	16.0	0.0436	2.66
1136/1-150	206	212.6	212.0	0.1741	0.82
1136/1-550	39	45.4	42.0	0.1240	2.89
1136/3-150	114	76.7	78.0	0.1656	2.16
1136/3-550	25	23.2	23.0	0.0389	1.71

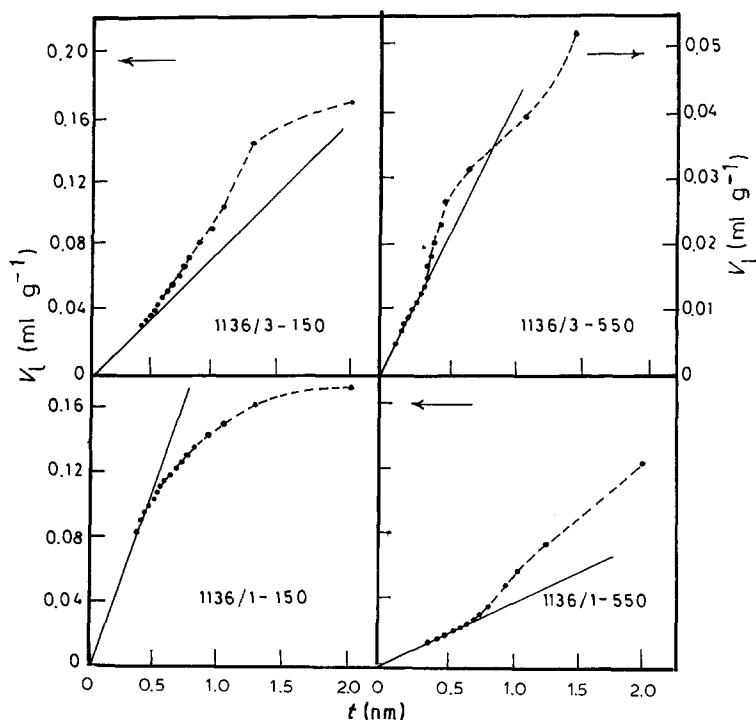


Figure 7 V_t - t plots obtained from nitrogen adsorption data on the heated products of samples 1136/1 and 1136/3.

markedly affects the narrower pores at the expense of the wider ones.

The V_t - t plots of the products of rutile Tr are quite different from those of anatase Ta (Fig. 6) which is believed to consist essentially of minute elemental particles much smaller than those of rutile that impart to it the observed high specific area. The rutile products are generally characterized by possessing a wider pore system than those from anatase. The general shape of the V_t - t plot of sample Tr-150 does not actually indicate the predominance of micropores but emphasizes the existence of some micropores together with a pore system having sizes of limited dimension that does not permit capillary condensation. The increase in slope at $t \approx 1.08$ nm ($p/p^0 = 0.85$) shows that condensation takes place at $p/p^0 > 0.85$ as reflected by the adsorption isotherm. The absence of a hysteresis loop in this sample shows that the condensation-evaporation process is not hindered, but takes place freely as does that in tapering pores. It thus seems that at $p/p^0 < 0.85$ the "internal" surface or that between the elemental particles adsorbs the nitrogen and at $p/p^0 > 0.85$ it is the outer parts that become occupied, i.e. that between the secondary particles (group of elemental particles).

Samples Tr-250 and Tr-400 point clearly to the predominance of mesoporosity and to the presence of two groups of mesopores. The marked increase in crystallite size observed above 400°C (Fig. 4) seems responsible for the disappearance of the group of pores in the narrower thickness range, where at 500°C , only one group of mesopores is observed by the upward deviation at $t \approx 0.62$ nm.

It seems reasonable to conclude that the Bayer samples, whether Ta or Tr, are formed of particles each of which is actually constructed of many particulates or granules. It is essentially the size of these elemental particulates together with the size of their particles (aggregates) that determine not only the sur-

face texture but also the amount of physically adsorbed water.

Pore structure analysis of the Tioxide samples show the anatase sample 1136/1 to be predominantly microporous at 150°C but becomes completely mesoporous at 550°C with an average pore radius of 2.9 nm. The reverse is true for the rutile sample 1136/3 which is shown from its V_t - t plot to be completely mesoporous and thermal treatment at 550°C brings about some narrowing of the pores probably resulting from an expansion of the crystal lattice (Fig. 7).

3.2.2. Cyclohexane and benzene adsorption

Full adsorption-desorption cycles of cyclohexane and benzene at 35°C are obtained for the thermally treated products of both modifications from Bayer and Tioxide. In all cases the adsorption isotherms obtained by both vapours are type II and are completely reversible, emphasizing the absence of capillary condensation, except for the benzene adsorption on the Tioxide anatase samples that exhibited closed hysteresis loops with relative pressure closures ≥ 0.7 .

Surface areas are evaluated from the isotherms by the use of the BET equation adopting a value of $A_m = 0.39$ nm² (flat orientation) [32] for cyclohexane for all samples except 1136/1-150 and 1136/3-550, where a value of 0.30 nm² (vertical orientation) [32] was used because the former gave areas that are comparable or higher than the nitrogen areas in spite of the presence of micropores in these samples and of the larger molecular size of cyclohexane. A slanting orientation may occur as well and so the vertical orientation is employed here in order to give the lower area limit. In the case of benzene as adsorbate, the specific areas were computed by adopting a value of 0.25 nm² [32] for the molecular cross-sectional area where the molecule is oriented with the longer axis perpendicular to the surface otherwise equal or higher areas than those from nitrogen adsorption were obtained in

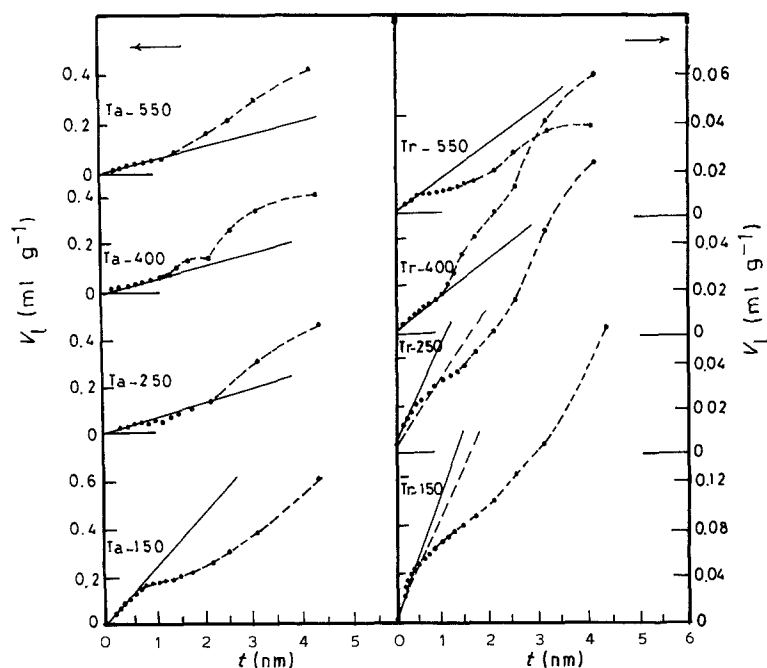


Figure 8 V_1-t plots obtained from cyclohexane adsorption data on the dehydrated products of samples Ta and Tr.

many cases. The cyclohexane and benzene molecules seem to measure only a fraction of the total area measured by nitrogen (Tables III and IV, column 7, respectively). The fraction of area measured by benzene is, in most cases, smaller than that measured by cyclohexane except distinctly for sample Ta-250 which seems to possess pores that permit the passage of the benzene molecules more than those of cyclohexane. The accessibility of the pores to benzene molecules is controlled not only by the size parameter but also by the weak interactions that may occur between the adsorbate benzene molecules and the surface that are absent with cyclohexane.

A large decrease in specific surface area, as obtained from cyclohexane, is observed upon heating samples Ta and Tr to 250°C, being more significant for the former. Above 250°C, the area changes are negligible for the anatase samples whereas for rutile a small gradual decrease is observed. In the case of Ti oxide samples cyclohexane has a comparable area to nitrogen for the rutile samples only, whereas lower values are produced for the anatase samples. It is clear from nitrogen adsorption that these rutile samples possess wider pores and so sample 1136/1-550 is predominantly mesoporous. Thus the inaccessibility of the anatase

samples to cyclohexane molecules can be understood for sample 1136/1-150 which is predominantly microporous (from nitrogen adsorption), but for the mesoporous sample 1136/1-550 it is quite ambiguous — the cross-sectional area occupied by cyclohexane on this sample seems to exceed 0.39 nm², probably arising from a stretching or expansion of the molecule in the flat orientation resulting from hydrogen bonding with the oxygen of the acidic hydroxyls. Thus cyclohexane measures a comparable area to nitrogen for the rutile (T) samples — about 90% to 99% of the nitrogen areas — whereas it measures only ~60% of nitrogen areas in the case of the anatase (T) samples.

The V_1-t plots constructed for pore structure analysis using the cyclohexane adsorption data are achieved by use of the t -curves of Mikhail and Shebl [34]. The pore analyses for samples from Ta show that the pores are predominantly microporous for the sample heated at 150°C and mesoporosity increases with increasing treatment temperature. Sample Ta-400 shows the presence of two groups of pores, one group seems to arise from an inner pore system, whereas the other observed at a higher t -value results from those formed between the grains (Fig. 8). This was not revealed by nitrogen adsorption where the small molecular

TABLE III Some surface characteristics of the heated products of Ta, Tr, 1136/1 and 1136/3 as obtained from cyclohexane adsorption

Sample	BET C-constant	A_m nm ²	$S_{BET}^{C_6H_{12}}$ (m ² g ⁻¹)	$S_t^{C_6H_{12}}$ (m ² g ⁻¹)	$V_{p0.95}$ (ml g ⁻¹)	$S_{BET}^{C_6H_{12}}/S_{BET}^{N_2}$
Ta-150	14.0	0.39	234.6	235.0	0.6520	0.92
Ta-250	17.0	0.39	55.9	60.0	0.4730	0.35
Ta-400	29.0	0.39	55.7	59.0	0.4350	0.75
Ta-550	24.0	0.39	48.1	49.0	0.4260	0.86
Tr-150	18.0	0.39	91.8	110.0	0.2480	0.84
Tr-250	18.0	0.39	32.2	46.0	0.2070	0.72
Tr-400	37.0	0.39	14.3	16.5	0.1870	0.52
Tr-550	25.0	0.39	13.8	15.5	0.1210	0.95
1136/1-150	46.0	0.30	125.1	—	0.4250	0.59
1136/1-550	54.0	0.39	27.8	—	0.4440	0.61
1136/3-150	12.0	0.39	75.9	74.0	0.4010	0.99
1136/3-550	13.0	0.30	20.8	19.0	0.3530	0.90

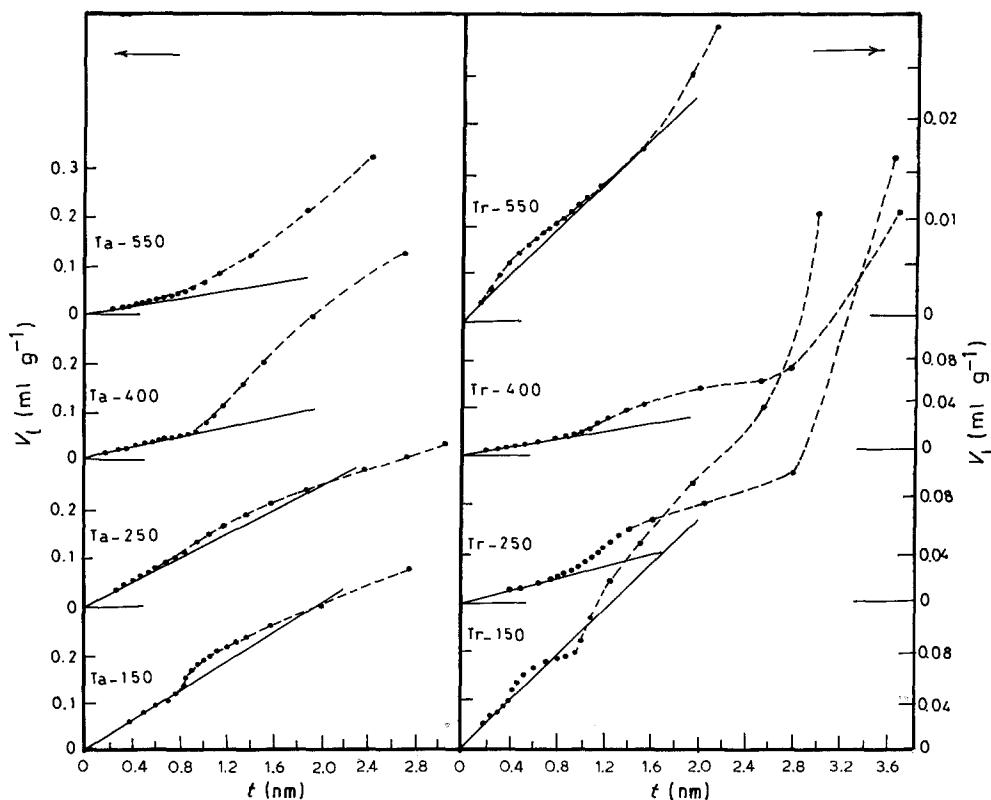


Figure 9 V_t - t plots obtained from benzene adsorption data of the dehydrated products of samples Ta and Tr.

dimension of nitrogen does not permit such a differentiation. Pore analysis of the products from Tr is achieved for those heated at 400 and 550°C only where agreement with the $S_{\text{BET}}^{\text{C}_6\text{H}_{12}}$ is observed, but for samples heated at lower temperatures a deviation reaching ~40% is observed. If the slope necessary to give a correct S_t estimate for these low-temperature samples is drawn (dashed line), then the points at low t -values fall above the straight line. This may indicate some sort of specific interaction, probably between the hydrogen of cyclohexane and the oxygen of the rutile samples. Differences in the a and c dimensions of the crystal lattice as observed for the anatase and rutile samples heated at these two temperatures (150 and 250°C) may be responsible for supplying a reasonable spacing between the oxygen of the hydroxyls for interaction with the cyclohexane, if it actually occurs. However, although the cyclohexane molecule possesses the same tendency for attraction to the silica surface as does nitrogen [35], its tendency for attraction to the titania surface is not known.

At 400°C the pores are completely mesoporous whereas at 550°C they are predominantly microporous, where shrinkage of the pores due to the expansion of the unit cell takes place.

No V_t - t plots could be constructed for the anatase (T) samples where, by comparison with $S_{\text{BET}}^{\text{C}_6\text{H}_{12}}$, deviations exceeding 30% were observed for both samples 1136/1-150 and 1136/1-550. However, good agreement with $S_{\text{BET}}^{\text{C}_6\text{H}_{12}}$ was observed for the corresponding rutile samples. They both showed a downward deviation commencing at t -values of ~0.7 and ~0.4 nm for samples 1136/3-150 and 1136/3-550, respectively, pointing to the narrowing of the pores upon heating to 550°C as previously observed from nitrogen adsorption. The decrease in slope does not continue in both plots but increases again where some mesopores manifest their presence. The pores of these two samples are thus predominantly microporous with respect to cyclohexane. In the detection of porosities from benzene adsorption the t -curves of Mikhail and co-workers [34, 36] and Khalil [37] are

TABLE IV Some surface characteristics of the heated products of Ta, Tr, 1136/1 and 1136/3 obtained from benzene adsorption

Sample	BET C-constant	$S_{\text{BET}}^{\text{C}_6\text{H}_6}$ ($\text{m}^2 \text{g}^{-1}$)	$S_t^{\text{C}_6\text{H}_6}$ ($\text{m}^2 \text{g}^{-1}$)	$V_{p0.95}$ (ml g^{-1})	$S_{\text{BET}}^{\text{C}_6\text{H}_6}/S_{\text{BET}}^{\text{N}_2}$
Ta-150	66.0	148.0	148.0	0.4980	0.58
Ta-250	15.0	112.7	120.0	0.5020	0.71
Ta-400	27.0	45.9	50.0	0.5580	0.62
Ta-550	33.0	34.1	33.0	0.4860	0.61
Tr-150	12.0	96.0	97.0	0.4540	0.88
Tr-250	41.0	24.9	23.8	0.2750	0.56
Tr-400	13.0	15.4	10.0	0.1750	0.55
Tr-550	8.0	11.8	10.8	0.1590	0.72
1136/1-150	146.0	115.7	112.0	0.4180	0.54
1136/1-550	9.0	31.0	28.5	0.3350	0.68
1136/3-150	72.0	46.6	48.0	0.5380	0.61
1136/3-550	150.0	13.0	14.0	0.1310	0.56

employed where good agreement between S_t and S_{BET} is observed for all samples (Table IV, columns 4 and 3, respectively). From the V_t-t plots of the heated Ta anatase products it is clear that at 150 and 250°C, the samples are predominantly mesoporous with the existence of some micropores (Fig. 9). However, at 250°C some widening has occurred at the expense of other neighbouring pores permitting the entrance of benzene into pores that were previously inaccessible thus increasing the area ratio $S_{\text{BET}}^{\text{C}_6\text{H}_6}/S_{\text{BET}}^{\text{N}_2}$ to 0.71. It seems that when cyclohexane was employed, the molecules become inaccessible to these neighbouring pores that previously (at 150°C) were wide enough to permit the entrance of the cyclohexane molecules, resulting in a marked decrease in the measured area. At temperatures > 250°C the samples become completely mesoporous relative to the benzene molecules.

In the pore analysis of the Tr-products, sample Tr-150 gave a peculiar plot where an upward deviation was observed at $t = 0.4$ nm which reverts back and cuts the straight line at $t = 0.72$ nm, then increases again to cut the straight line at 1.08 nm, giving a zigzag-like structure (Fig. 9). It may be that the increased force field arising from the opposite walls of a certain pore group (double-wall effect) [38] as well as the presence of the π bonds of the adsorbate causes a denser uptake of the benzene molecules. However, the sample is characterized to contain both meso- and micropores. Samples heated at 250 and 400°C are completely mesoporous. Heating at 550°C increases the accessibility of benzene to penetrate into the pore system and the V_t-t plot shows an upward deviation at $t \approx 0.4$ nm — this reflects the enhanced adsorption resulting from the forces arising from the π bonding in benzene. Widening of the pore system at this temperature increases the area ratio to 0.72 (Table IV, column 6).

The anatase 1136/1(T) sample is found to be predominantly microporous at 150°C. This microporosity completely disappeared at 550°C. For the rutile sample 1136/3, the products obtained at 150 and 550°C are completely mesoporous, the latter possessing smaller pore dimension than the former.

Both Ti oxide modifications heated at 150°C show the presence of two groups of pores of different sizes.

References

1. M. E. WINFIELD, in "Catalysis", edited by P. H. Emmett, Vol. 7 (Reinhold, New York, 1960) p. 23.
2. G. K. BORESKOV, *Disc. Faraday Soc.* **41** (1966) 263.
3. P. C. GRAVELLE *et al.*, *ibid.* **52** (1971) 140.
4. G. MUNUERA and F. S. STONE, *ibid.* **52** (1971) 205.
5. F. S. STONE, *Anal. Real Soc. Espan. Fis. Quim.* **61** (1965) 109.
6. M. R. HARRIS and G. WHITAKER, *J. Appl. Chem.* **12** (1962) 490.
7. *Idem, ibid.* **13** (1963) 198.
8. S. J. TEICHNER *et al.*, *Adv. Colloid Interface Sci.* **5** (1976) 245.
9. J. RAGAI and K. S. W. SING, *J. Chem. Technol. Biotechnol.* **32** (1982) 988.
10. *Idem, J. Colloid Interface Sci.* **101** (1984) 369.
11. C. MORTERRA, A. CHIORINO and A. ZECCHINA, *Gazzetta Chimica Italiano* **109** (1979) 683.
12. *Idem, ibid.* **109** (1979) 691.
13. K. TANABE *et al.*, in "Preparation of Catalysts", edited by B. Delmon, P. A. Jacobs and G. Poncelet (Elsevier, Amsterdam, 1976) pp. 65-74.
14. A. KUROSAKI and S. OBAZAKI, *Nippon Kogaku Kaishi* **12** (1976) 1816.
15. J. V. SMITH (Ed.), "X-ray Powder Data File and Index to X-ray Data File" (American Society for Testing and Materials, Philadelphia, Pennsylvania, 1961).
16. Powder Diffraction File ASTM Alphabetical Index of Inorganic Compounds (International Center of Diffraction Data, Pennsylvania, 1978).
17. J. M. VLEESKENS, PhD thesis, Delft University of Technol. (1959).
18. CH. A. PHILIP, PhD thesis, Faculty of Science, Ain Shams University (1985).
19. P. JONES and J. A. HOCKEY, *Trans. Faraday Soc.* **67** (1971) 2669.
20. H. P. BOEHM and M. HERRMANN, *Z. Anorg. Allg.* **352** (1967) 156.
21. S. A. SELIM *et al.*, *Thermochim. Acta* **45** (1981) 349.
22. M. PRIMET, P. PICHAT and M. V. MATHIEU, *J. Phys. Chem.* **75** (1971) 1216.
23. H. P. BOEHM, *Disc. Faraday Soc.* **52** (1971) 264.
24. T. L. WEBB, in "Differential Thermal Analysis" Vol. 1, edited by R. C. Mackenzie (Academic Press, London, 1970) p. 244.
25. H. LIPSEN and H. STEEPLE, in "Interpretation of X-ray powder Diffraction Patterns" (Macmillan, London, 1970).
26. S. R. YOGANARASIMHAM and C. N. R. RAO, *Trans. Faraday Soc.* **58** (1962) 1579.
27. B. C. LIPPENS, J. H. DE BOER and B. G. LINSEN *J. Catal.* **3** (1964) 32.
28. J. H. deBOER, B. C. LINSEN and TH. J. OSINGO, *ibid.* **4** (1965) 643.
29. R. SH. MIKHAIL, N. M. GUINDY and S. HANAFI, *J. Chem. A.R.E., Special Issue Tourky* **53** (1973).
30. J. D. CARRUTHERS *et al.*, *Chem. Ind.* (1968) 1772.
31. R. W. CRANSTON and F. A. INKLEY, *Adv. Catal.* **9** (1957) 143.
32. R. N. SMITH, C. PIERCE and H. CORDES, *J. Amer. Chem. Soc.* **72** (1950) 5595.
33. R. M. BARRER and J. S. S. REAY, in "Proceedings of the Second International Congress on Surface Activity", Vol. 2 (Butterworths, London, 1957) p. 79.
34. R. SH. MIKHAIL and F. A. SHEBL, *J. Colloid Interface Sci.* **32** (1970) 505.
35. R. S. McDONALD, presented at the Pittsburgh Conference on "Analytical Chemistry and Applied Spectroscopy", 2 March (1956).
36. R. SH. MIKHAIL, S. A. SELIM and F. A. SHEBL, *Egypt J. Chem.* **19** (1976) 405.
37. A. M. KHALIL, *Thermochim. Acta* **36** (1980) 225.
38. S. J. GEGG and K. S. W. SING, in "Adsorption Surface Area and Porosity" (Academic Press, London, 1967) p. 201.

Received 8 June

and accepted 1 December 1989